Migration of Antifog Additives in Agricultural Films of Low-Density Polyethylene and Ethylene-Vinyl Acetate Copolymers

L. Irusta,[1] A. González,[1] M. J. Fernández-Berridi,[1] J. J. Iruin,[1] J. M. Asúa,[1] I. Albizu,[1] A. Ibarzabal,[1] A. Salmerón,[2] E. Espi,[2] A. Fontecha,[2] Y. García,[2] A. I. Real[2]

[1]*Department of Polymer Science and Technology and Institute for Polymer Materials (POLYMAT), University of the Basque Country, 20080 San Sebastian, Spain*
[2]*Repsol YPF Centre of Technology, 28931 Móstoles, Madrid, Spain*

Received 1 February 2008; accepted 4 September 2008
DOI 10.1002/app.29280
Published online 18 November 2008 in Wiley InterScience (www.interscience.wiley.com).

ABSTRACT: In this work, polymer films of low density polyethylene and ethylene-vinyl acetate copolymers containing two types of antifog additives (nonionic surfactants) were exposed to two simulated horticultural greenhouse environments, reproducing hot and cold climate conditions. The evolution of the antifog effect was visually observed and that of the additive concentration measured using Fourier transform infrared spectroscopy (FTIR). All the films studied showed good antifog properties, but in all cases, the duration of the antifog effect was longer in the hot-climate test. From the FTIR, we can conclude that the additives studied showed a low migration rate and, therefore, when the antifog effect is lost, important quantities of the additive remain in the bulk. © 2008 Wiley Periodicals, Inc. J Appl Polym Sci 111: 2299–2307, 2009

Key words: antifog additive; nonionic surfactant; agricultural film; greenhouse; FTIR

INTRODUCTION

Agricultural films are widely used as greenhouse cover. Their use is increasing in hotter climates to assist water conservation and to improve the efficiency of crop production.

Normal polyethylene films used in greenhouses have no affinity with water. The water that condenses forms round droplets because this is the shape that minimizes the contact area between the water and the film. The reason why water condenses in that form is the difference between the surface tensions of the water and the hydrophobic polymer.[1] These droplets reduce the light transmission and will often "rain" down inside the greenhouse resulting in physical damage to plants as well as increasing the risk of disease.[2]

To solve this problem, the wettability of the polymer surface must be improved. This wettability can be modified by several surface treatment techniques or by adding tensoactive agents (antifog additives) that migrate to the surface to modify the surface tension. It is clear that a permanent surface treatment,[3] such as making some micro or nano structure on it would be the best solution, but the addition of tensoactives implies minor technological difficulties when obtaining the polymeric film.

The addition of tensoactives is probably not the best solution to increase the wettability of a surface but it is surely preferred by the industry because it implies lower costs. When the tensoactives (surfactants) are incorporated into the polymer matrix, they migrate to the surface of the film, increasing its surface tension. At the same time, a small quantity of the surfactant dissolves in the water droplets, decreasing the surface tension of the water. At one point, both surface tensions become similar and water spreads into a continuous layer on the surface of the film and does not reflect the sunlight. This is called "antifog" effect.[4] The role of the additive is not to prevent water deposition on the film but to condense it into an invisible continuous thin layer. Nevertheless, the effect of the surfactant is not permanent, and the film loses the antifog effect after some weeks or months.

To achieve the antifogging property, the additive needs to be present on the surface of the polymer. Therefore, the migration properties of the additive from the bulk of the film to the surface are crucial parameters. Moreover, when the film is used in greenhouse environment, there is a continuous loss of the additive as some dissolves in the surface water. In this situation, the choice of the additive must take into account a suitable migration rate and

Correspondence to: L. Irusta (lourdes.irusta@ehu.es).
Contract grant sponsor: CENIT Mediodia project (CSIC).

a low solubility in water that give rise to an adequate surface concentration for a maximum time period.

Antifogging additives are typically surface-active products made of two main parts: a hydrophilic head and a lipophilic tail. Examples include sorbitan, glycerol, polyglycerol, and polyoxyethylene esters. The parameters that must be considered when selecting the antifog agents for agricultural films include the type of polymer and the temperature at which the film will be used.

Although the importance of these parameters in the antifog effect durability is clear, there is little literature data that relate the antifog effect durability to the film composition as well as to the service temperature.[5–7] The literature data show that, in polyethylene, the migration rate of the antifog additive decreases when the additive size increases.[8] Moreover, when the crystallinity of polyethylene is increased, the migration rate of the additive to the surface increases. Nevertheless, to our knowledge, literature does not contain similar studies with ethylene/vinyl acetate copolymers, often used as greenhouse covers. On the other hand, the effect of the service temperature on the antifog property has not been clearly established.

In the study presented in this article, the effectiveness of two antifog additives (fatty acid glycerol monoester and *N*-stearyl diethanol amine fatty acid monoester) was compared in different compositions of low density polyethylene (LDPE) and ethylene/vinyl acetate (EVA) copolymer films. Two different simulated greenhouse environments reproducing both hot-climate and cold-climate conditions were used to establish the effect of the service temperature in the durability of the antifog effect.

EXPERIMENTAL

Materials

Two nonionic surfactants were studied: additive AAG-01 is a fatty acid glycerol monoester (glycerol monostearate) and additive AAG-02 a *N*-stearyl diethanol amine fatty acid monoester (Stearyldiethanolamine monostearate). The two additives were supplied by Repsol YPF (Madrid, Spain). Low density polyethylene (LDPE Alcudia PE-033), and ethylene vinyl acetate copolymers (EVA Alcudia PA-500, PA-530 and PA-570, having 4, 9, and 14 wt % vinyl acetate, respectively) were supplied by Repsol YPF (Madrid, Spain).

Twenty films with different compositions (Table I) were obtained by extrusion in a twin-screw extruder Werner and Pfleiderer ZSK-30 and subsequent film blowing in a Dr. Collin monolayer lab-scale equipment. The films were blown to a thickness of 200 μm. All the films contained 2 wt % of mineral filler. The mineral filler used was calcined kaolin PoleStar 200R supplied by Imerys (Paris, France).

TABLE I
Nomenclature and Composition of the Blown Films

Nomenclature	wt % VA	wt % AAG-01	wt % AAG-02
POL-01	0	0	0
POL-02	0	1	0
POL-03	0	2	0
POL-04	0	0	1
POL-05	0	0	2
POL-06	4	0	0
POL-07	4	1	0
POL-08	4	2	0
POL-09	4	0	1
POL-10	4	0	2
POL-11	9	0	0
POL-12	9	1	0
POL-13	9	2	0
POL-14	9	0	1
POL-15	9	0	2
POL-16	14	0	0
POL-17	14	1	0
POL-18	14	2	0
POL-19	14	0	1
POL-20	14	0	2

Antifog tests

Polymer film samples were placed as the cover of a laboratory thermostatic water bath. A constant water level was maintained, and the atmosphere between the film and the water bath was assumed to be saturated with water vapor. In the hot-climate test, the water temperature in the bath was 50°C, the laboratory temperature was 23°C, and the temperature in the space between the film and the water bath was 40°C. In the cold-climate test, the water bath was enclosed in a climatic chamber where temperature oscillated between 5 and −5°C every 12 h. The water bath temperature was 30°C, and the temperature in the space between the film and the water bath was 20°C.

The effectiveness of the antifog effect was evaluated by visual inspection of how water condensed on the inner films surface using proprietary ratings from B to E (Fig. 1). Rating E indicates complete transparency and no visible traces of water on the film. Performance then decreases gradually toward a B rating, indicating 100% small discrete droplets. An acceptable antifog effect was considered when at least 50% of the surface of the film showed C, D, or E ratings.

Characterization

The infrared measurements were recorded on a Nicolet spectrometer, Magna 560 FTIR model, at a resolution of 2 cm^{-1}. The signal was averaged from

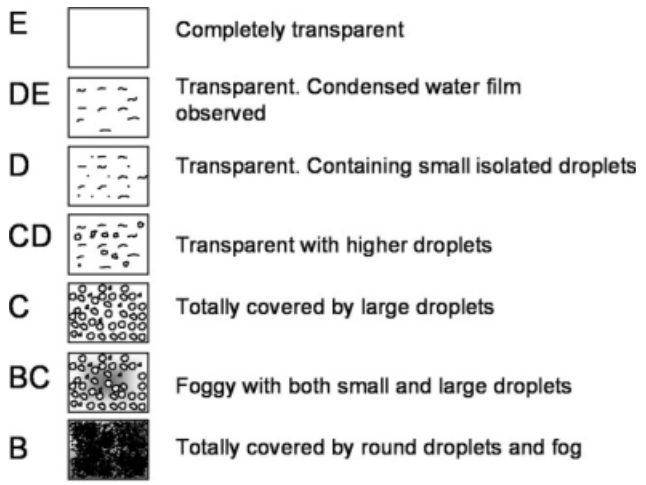

Figure 1 Qualitative range of the antifog effect quality.

a minimum of 64 scans. Attenuated total reflectance (ATR) experiments were carried out using an ATR objective (Spectra Tech) with a zinc selenide crystal mounted on a microscope (Spectra Tech) attached to the FTIR spectrometer. A MCT detector was used.

Water content and the hydroxyl number of the additives were measured according to ASTM E203-01 and D 4274-99, respectively.

The melting point of the additives was measured in a Perkin–Elmer Pyris 1 DSC calorimeter.

The solubility of the additives was calculated at 25 and 50°C. For these measurements, 1 g of the additive was added to 100 mL of distilled water under magnetic stirring. The dispersion was immersed in a thermostatic bath at the desired temperature (25 or 50°C) and maintained for 1 h under stirring. After that, the dispersion was filtered using gravimetric paper and the solid was dried in an oven at 50°C until constant weight.

RESULTS AND DISCUSSION

Characterization of the additives

The results of the respective additives characterized using the above-mentioned techniques are shown in Table II.

Water contents of the two additives were very similar, but the hydroxyl number and melting point of AAG-02 were lower than those of AAG-01.

The solubility of both additives in water at 25 and 50°C was low. Moreover, at 25°C, AAG-02 solubility was lower than that of AAG-01. This fact can be related to the lower hydroxyl number of AAG-02. Nevertheless, at 50°C, the solubility of AAG-02 increases considerably, becoming higher than that obtained in AAG-01 at the same temperature. This can be explained as a consequence of the molten state of this additive at this temperature.

Infrared calibration

FTIR spectra of all the samples were recorded using two different methods. In the first one, the spectra were registered in transmission mode to use them in the determination of the total (bulk) additive concentration. The spectra used to calculate the surface additive concentration were registered in the attenuated total reflectance (ATR) mode.

Figure 2 shows the absorption FTIR spectra of the two additives and those of the film samples containing 14 wt % of vinyl acetate (VA) without additive (POL 16), with 2 wt % of AAG-01 (POL 18), and with 2 wt % of AAG-02 (POL 20).

The spectra of the two additives are very similar. They are mainly characterized by the hydroxyl stretching vibration (3400 cm^{-1}), the carbonyl stretching at 1730 cm^{-1}, and different C—O stretching vibrations between 1000 and 1300 cm^{-1}. Additive AAG-01 shows a higher relative intensity of the OH stretching vibration (Area OH/Area C—H at 3000 cm^{-1}) that can be related to the higher value of its hydroxyl number (experimentally measured).

The FTIR absorption spectra of the films present saturation problems due to film thickness. The spectrum of the sample containing 14 wt % of VA (POL 16) shows the characteristic bands of this polymer (carbonyl stretching at 1735 cm^{-1}, and C—O stretching between 1000 and 1300 cm^{-1}). Taking into account these assignments, it is clear that the spectra of both additives present large overlapping with the spectrum of the pure polymer. This fact is clearly shown in the spectra of samples containing 2 wt % of additive (POL 18 and POL 20) where no bands attributable to the additive can be observed.

To perform a classical quantitative analysis, using Beer's law, the ideal situation is to locate an isolated absorption band of the additive in question, and to

TABLE II
Characterization of the Additives

Additive	% water (wt %)	Hydroxyl number (mg of KOH/g)	Solubility 25°C (g/L)	Solubility 50°C (g/L)	Melting point (°C)
AAG-01	1.1	247	0.10	0.21	55
AAG-02	1.0	136	0.07	0.36	42

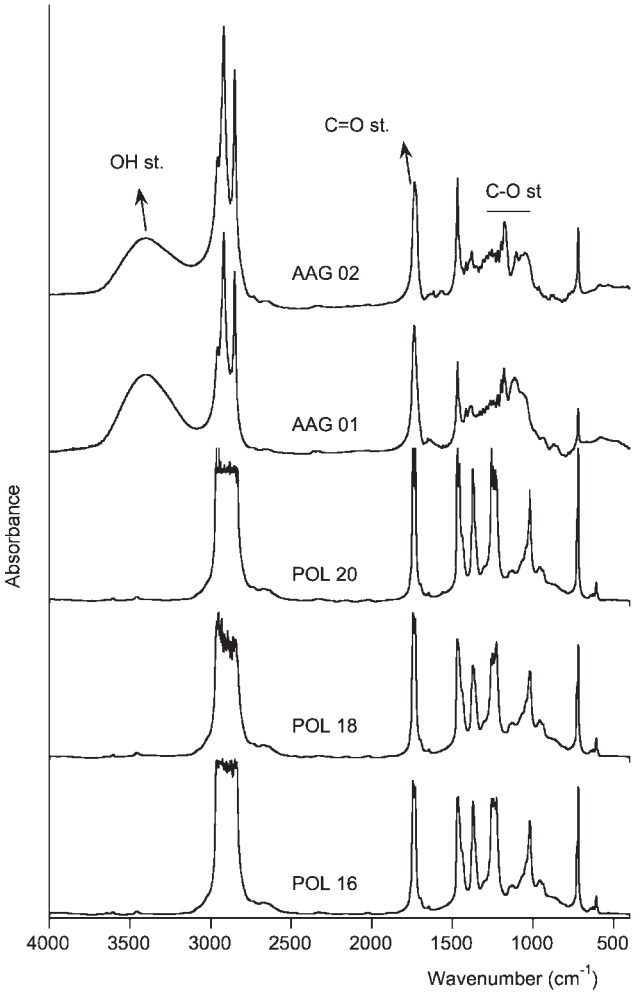

Figure 2 FTIR absorption spectra of AAG-01, AAG-02, POL 16, POL 18, and POL 20.

extract the relevant intensity information by peak height or peak area. Modern spectroscopic practice has progressed far beyond the use of Beer's law to relate the absorbance of an analyte at a characteristic wavelength to the concentration of that analyte, but it is still the basis of modern methods. To allow accurate analysis, a variety of sophisticated mathematical techniques have been developed that attempt to extract the analytical information from the spectroscopic data. One of these methods is the partial least squares method (PLS) that was used in this work. This method is described at the end of this section.

FTIR-ATR spectroscopy was used to obtain the surface spectra. Figure 3 shows the ATR spectra of the two additives and the spectra of the film samples containing 14 wt % of VA without additive (POL 16) and with 2 wt % of AAG-01 (POL 18) and 2 wt % of AAG-02 (POL 20). As expected, the same overlapping observed in the transmission mode spectra is also present here, so the PLS method was also selected to perform the quantitative analysis. However, it is well known that in ATR spectroscopy, the penetration depth has wavenumber dependence,[9] a fact that makes the quantitative analysis difficult. In this work, ATR measurements were performed using a ZnS crystal with an angle of incidence of 45°. Considering that the refractive index of EVA is near 1.5, the penetration depth is about 0.6 μm at 3333 cm^{-1} and about 2 μm at 1000 cm^{-1}. Nevertheless, in the region selected to perform the quantification (1270–970 cm^{-1}), the depth changes from 2 to 1.6 μm, so, to perform the quantitative analysis, no depth change was considered.

For the quantification of the additive concentration, a commercial computer program (Turbo Quant Analyst, Nicolet) was used. Partial least squares (PLS)[10] method was used where three PLS factors were taken. In the transmission spectra, due to the film thickness and, therefore, to detector saturation problems, the less absorbing regions (1170–1067 cm^{-1} and 2700–1936 cm^{-1}) were selected for both additives. However, in ATR experiments, as there are no thickness limitations, any spectral region can be suitable. In this case, the 1270–975 cm^{-1} region

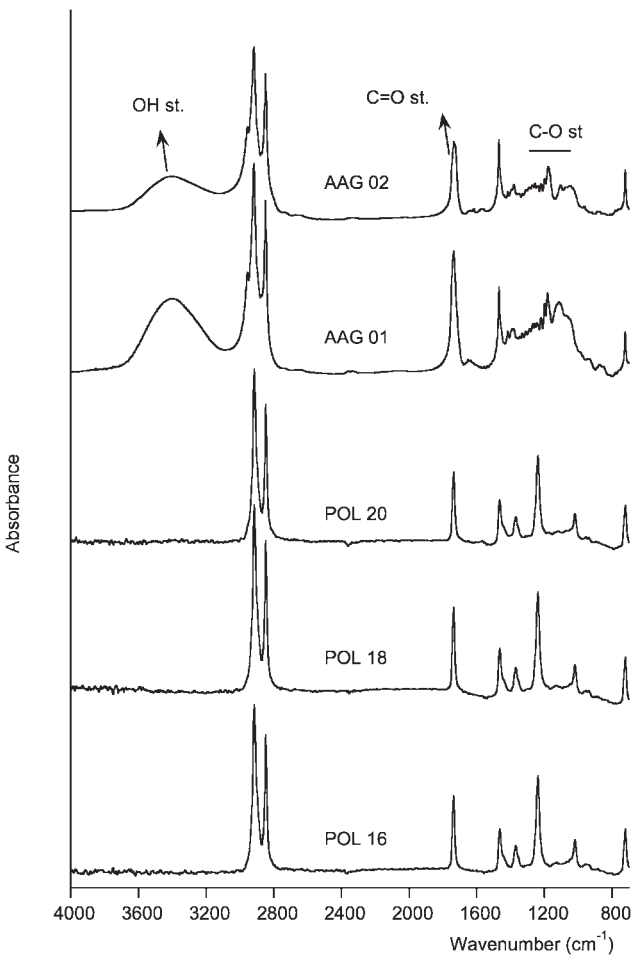

Figure 3 FTIR ATR spectra of AAG-01, AAG-02, POL 16, POL 18, and POL 20.

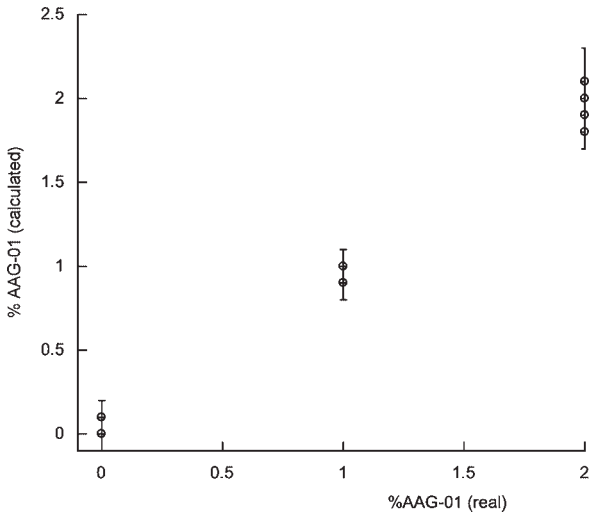

Figure 4 Calibration plot for AAG-01 in transmission mode.

was selected for both additives to create an accurate method. In all the cases, the path length of the samples was corrected using internal reference. According to this, four different quantitative methods were obtained for additives AAG-01 and AAG-02 in transmission mode or ATR. In all cases, three spectra, at different points in the sample, were recorded to characterize each polymer film. The three spectra displayed similar intensities; two of them were used in the PLS calibration and the other was used for validation. Figure 4 shows, as an example, the real and calculated concentration of AAG-01, using one of the calibration methods. As can be seen, the calculated values are in good agreement with the real composition of the samples. Nevertheless, the standard deviation of the data is around 0.1 in all the samples.

Simulated greenhouse experiments

All the films were exposed to the two simulated greenhouse environments that have been previously described, one for hot and the other for cold climate. The experiment was concluded once it was observed that the film did not show antifog characteristics, according to the previously defined criteria. Table III resumes the duration of the antifog effect in the studied samples.

According to the results shown in Table III, all the films containing additives (AAG-01 or AAG-02) showed antifog effect demonstrating that the two additives impart antifog properties to the polymer samples. The same result has been obtained in literature.[5] However, the effect is not permanent and disappears after a time period that depends on film composition as well as on the test conditions. The duration of the antifog effect increases with the additive concentration.

As previously mentioned, to get the antifog effect, the additive must be present at the surface of the polymer film. Consequently, any loss of the antifog effect must be related to a decrease of its concentration in the surface. This concentration decrease would occur when the condensed water in the accelerated test "washes" the surface of the polymer film.

However, when the water present on the polymer surface dissolves some additive molecules, a concentration gradient is generated from the bulk film to its surface and additive migration starts. This migration would increase the additive surface concentration.

For the antifog effect to be long-lasting, the water dissolution rate and the additive migration rate must be conveniently balanced. If the additive water solution rate is higher with respect to the additive migration rate, the film will lose the antifog property because the surface additive concentration will be low, even though the additive concentration in the polymer bulk can still be high. On the contrary, if the additive migration rate is too high, the duration of the antifog property will depend exclusively on the additive water solubility. In the next section, we will try to evaluate the relative rate of these processes by FTIR spectroscopy.

Hot climate conditions

Samples taken at different exposure times in the hot climate test were analyzed by FTIR spectroscopy

TABLE III
Anti-Fog Properties Durability of the Studied Samples

Sample	Additive concentration (w)%		Anti-fog effect in hot climate (days)	Anti-fog effect in cold climate (days)
	AAG-01	AAG-02		
POL-01	0	0	0	0
POL-02	1	0	14	4
POL-03	2	0	28	4
POL-04	0	1	28	4
POL-05	0	2	84	7
POL-06	0	0	0	0
POL-07	1	0	28	4
POL-08	2	0	84	4
POL-09	0	1	7	4
POL-10	0	2	43	15
POL-11	0	0	0	0
POL-12	1	0	39	4
POL-13	2	0	61	4
POL-14	0	1	11	4
POL-15	0	2	54	22
POL-16	0	0	0	0
POL-17	1	0	54	4
POL-18	2	0	61	11
POL-19	0	1	11	11
POL-20	0	2	28	54

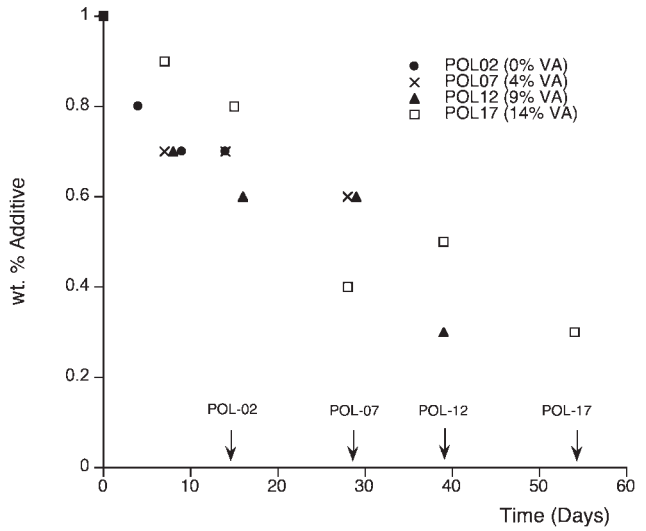

Figure 5 Concentration of additive AAG-01 versus time in the hot climate test for samples containing an initial value of 1%.

using transmission and ATR modes. The additive concentration was calculated using the previously defined calibration method. Three FTIR spectra were recorded to characterize each sample, and the additive concentration was calculated as the average of the values resulting from these measurements.

Figure 5 shows the total concentration of the additive at different exposure times under hot climate conditions, calculated by transmission FTIR spectroscopy for samples containing additive AAG-01 with an initial concentration of 1%. Taking into account that the final time has been defined as the time when the film does not show antifog effect any more, the evolution of the additive concentration as a function of exposure time was determined during different time periods. The final time for each sample is included in the graph.

Figure 6 shows the same calculation for samples containing an initial concentration of 2% of AAG-01 exposed to hot climate test.

From the observation of both figures, the following conclusions can be extracted:

Generally speaking, the total concentration of additive decreases with exposure time. There are a few data that do not follow this behavior, but taking into account the standard deviation obtained in the experiment ($\sigma_{n-1} \cong 0.1$), these values can be considered within the experimental error. Leaving aside these data, the decrease of the additive concentration shows similar values regardless of the polymer matrix composition. Taking into account that the data were obtained using a single additive (AAG-01) and that the solubility of the additive in water at the test conditions has a constant value, it can be concluded that the migration-rate of the additive is very similar in the different copolymers.

There is no relation between the total concentration of the additive and the antifog property of the film. For example, POL18 sample (Fig. 6), after 60 days of exposure, does not manifest any antifog property although it keeps 1% of the additive. However, all the samples initially containing 1% of the additive (Fig. 5) exhibit antifog properties. This observation suggests that the loss of the antifog property is related to the additive surface concentration and not to the total additive concentration diminution. As has been previously stated, to get a long lasting antifog property, the water dissolution rate and the additive migration rate must be conveniently balanced. The results show that the additive water solution rate is much higher than the additive migration rate, and therefore, the process is diffusion controlled. In other words, the concentration of the additive molecules in the surface will be determined by the rate of diffusion.

The data shown in the preceding paragraphs have manifested that the migration rate of additive AAG-01 is nearly the same for all the different EVA copolymers used as polymeric matrix, although the films have very different durability in the hot weather test. As the additive water solubility is a constant in the test, to explain the obtained results, it must be concluded that the initial additive surface concentration does not coincide with that of the bulk. It can be assumed that the initial surface concentration can be calculated by FTIR-ATR analysis. Nevertheless, FTIR is not an absolute technique; and to perform the quantitative analysis, it is necessary to assume that the surface concentration of the

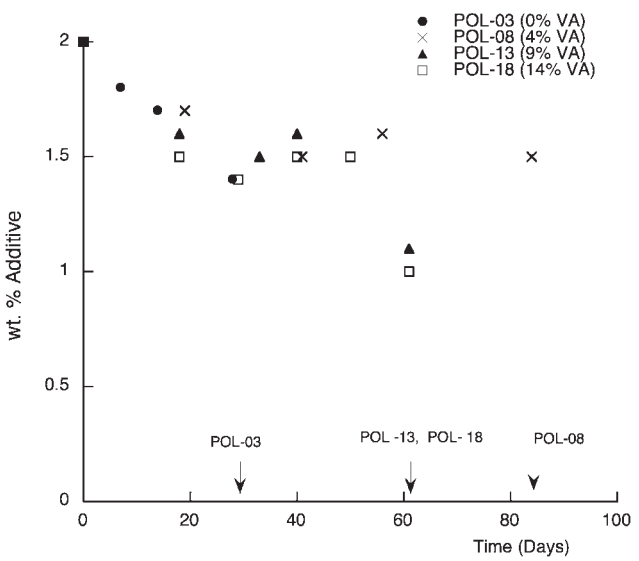

Figure 6 Concentration of additive AAG-01 versus time in the hot climate test for samples containing an initial value of 2%.

TABLE IV
Total and Surface Additive Concentration Relative Reduction at Failure Time in Hot Climate Conditions for Samples Containing Additive AAG-01

Sample	% Additive (formulation)	% Additive reduction (total, failure time)	σ_{n-1}	% Additive reduction (surface, failure time)	σ_{n-1}
POL02	1.0	30	10	60	20
POL07	1.0	40	10	50	30
POL12	1.0	70	0	50	20
POL17	1.0	70	10	90	40
POL03	2.0	25	10	0.0	40
POL08	2.0	25	0	75	30
POL13	2.0	45	0	70	10
POL18	2.0	50	10	100	20

additive matches the formulation composition. Therefore, from the results obtained by this technique, it is not possible to calculate the "real" initial additive surface concentration. Therefore, the ATR experiments cannot be used for the calculation of the initial surface additive concentration. However, the ATR data can be used as a measurement of the additive concentration evolution at different exposure times relative to the initial value. These results are shown in Table IV.

In the data shown in Table IV, it can be observed that the standard deviation obtained in the ATR measurements is higher than that obtained in the transmission experiments. These results can be due to a nonhomogeneous distribution of the additive on the surface, giving rise to a higher dispersion value.

Moreover, in the majority of the samples, the additive surface concentration reduction obtained in the ATR experiment is higher than the total additive concentration reduction obtained by transmission. Similar results have been obtained in literature for the migration of surfactants in polypropylene.[11] This result shows that the loss of the antifog property is related to the diminution of the additive surface concentration and not to the total additive concentration. To confirm this hypothesis, sample POL-18, that had lost the antifog effect after exposure to the accelerated test, was stored during a week at room temperature and without water condensation. After that time, the sample showed antifog property again. When the sample is stored, the migration of the additive continues but it is not extracted by water, so the additive concentration on the surface increases during storage.

Returning now to the data shown in Table III, samples containing additive AAG-02 show a lower duration in hot climate than samples containing additive AAG-01 (except sample POL-05). Figures 7 and 8 show the evolution of the additive concentration for samples containing additive AAG-02 at 1 and 2 wt %, respectively.

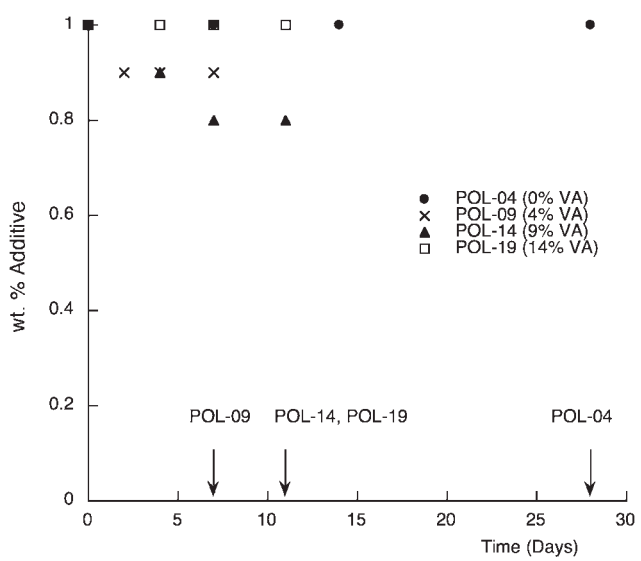

Figure 7 Concentration of additive AAG-02 versus time in the hot climate test for samples containing an initial value of 1%.

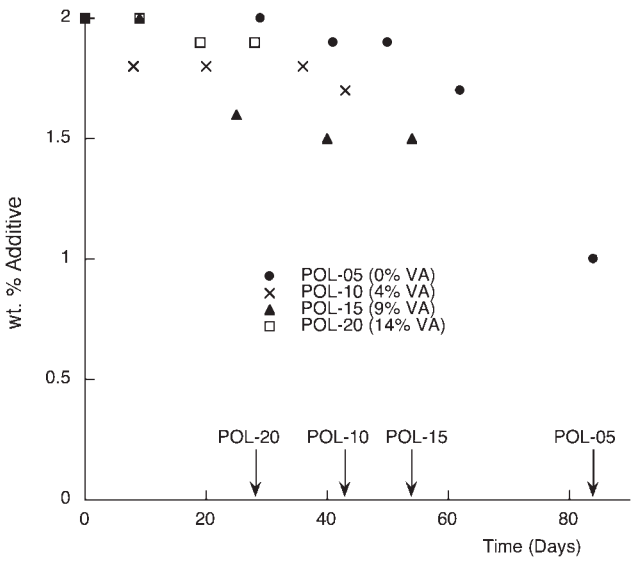

Figure 8 Concentration of additive AAG-02 versus time in the hot climate test for samples containing an initial value of 2%.

TABLE V
Total and Surface Additive Concentration Reduction at the Failure Time of the Hot Climate Test for Samples Containing AAG-02

Sample	% Additive (formulation)	% Additive reduction (total, failure time)	σ_{n-1}	% Additive reduction (surface, failure time)	σ_{n-1}
POL04	1.0	0	10	90	10
POL09	1.0	10	0	60	10
POL14	1.0	10	10	50	10
POL19	1.0	0	0	90	20
POL05	2.0	30	10	70	30
POL10	2.0	25	10	70	20
POL15	2.0	20	10	85	10
POL20	2.0	15	0	95	10

As can be seen in Figures 7 and 8, in almost all the samples, the total additive concentration decreases with exposure time. However, the reduction of the additive concentration is slightly lower than that obtained in samples containing additives AAG-01 (Figs. 5 and 6). According to this, the migration rate of additive AAG-02 is slightly lower than the rate of AAG-01. In literature,[8,11] the additives with lower molecular weight have shown greater mobility, so, the higher molecular weight of AAG-02 can explain its lower migration rate.

It is clear that as observed for AAG-01 containing samples, the loss of the antifog effect happens when samples contain important additive concentrations. The surface additive concentration reduction was calculated by FTIR-ATR spectroscopy, and the results obtained are shown in Table V.

In the data shown in Table V, the additive surface concentration reduction obtained in the ATR experiment is higher than the total additive reduction obtained in transmission mode. This result shows again that the loss of the antifog property is related to the additive surface concentration.

Finally, as has been previously stated, the duration of the antifog effect is shorter for samples containing additive AAG-02. According to the results obtained, this fact can be related to the higher solubility of AAG-02 at 50°C (Table II) as well as to its slightly lower migration rate.

Cold climate conditions

According to the data shown in Table III, the duration of the antifog effect is shorter in cold climate, except for sample POL-20. Leaving aside sample POL-20, the shorter duration of the antifog effect in cold climate could be attributed to two factors: a higher water solubility or a lower migration rate of the additives in the polymeric matrix.

TABLE VI
Total and Surface Additive Concentration Reduction at Failure Time in the Cold Climate Test for all the Samples

Sample	% Additive (formulation)	% Additive reduction (total, failure time)	σ_{n-1}	% Additive reduction (surface, failure time)	σ_{n-1}
POL02	1.0	10	0	0	30
POL03	2.0	5	0	45	60
POL04	1.0	0	0	30	30
POL05	2.0	0	10	25	40
POL07	1.0	10	10	0	30
POL08	2.0	0	10	50	20
POL09	1.0	0	0	40	10
POL10	2.0	0	10	45	10
POL12	1.0	10	0	10	10
POL13	2.0	10	50	85	30
POL14	1.0	0	10	40	10
POL15	2.0	0	10	80	0
POL17	1.0	10	0	10	20
POL18	2.0	15	10	45	30
POL19	1.0	0	0	50	30
POL20	2.0	0	0	80	20

In the cold weather test conditions, the film interior surface temperature is 20°C; meanwhile, in the hot climate test, this temperature is 40°C. As has been stated before (Table II), the water solubility of both additives increases with temperature. So, only taking this parameter into account, a higher duration of the antifog effect could be expected under cold conditions. However, in the cold weather test and due to the lower outside temperature, the amount of condensed water will be higher than that in the hot weather test. Therefore, the loss of additive as a consequence of its dissolution in water will be higher in the cold weather test, and this effect could give rise to a shorter duration of the antifog effect in this test.

As already mentioned, the migration-rate of both additives is the other factor that will affect the duration of the antifog effect. To study this effect, the FTIR results were analyzed. As the durability of the antifog effect in cold climate is very low, the evolution of the additive concentration with exposure time has not been included. Table VI shows the total and surface additive concentration reduction of the additives at failure time for all samples exposed to the cold weather test.

Generally speaking, the surface additive concentration reduction is higher than the total additive concentration reduction so, as in the hot weather test, the loss of the antifog property is due to a lowering of the surface additive concentration. In addition, the data clearly show that there is a very low variation of the total additive concentration with the exposure to the cold weather test, and the samples have almost the same composition initially and finally. It is also clear that the durability of the antifog effect is lower in the cold weather test. Moreover, the comparison between the remaining additive concentrations in both tests is not easy because the final failure times are very different. However, the relatively high duration of samples POL-15 and POL-20 in cold weather without total additive concentration variation gives us the possibility of considering that the migration rate of the additives in cold climate is very low compared to hot climate.

Taking into consideration all these parameters, the lower durability of the samples in cold climate is due to a combination of two factors: a higher water flow in the cold test that increases the washing of the polymer surface and a lower migration rate of the additive under these conditions.

Another interesting point that can be deduced from Table IV is that in the cold weather experiment, samples containing additive AAG-02 show a longer durability compared with those containing additive AAG-01. It is important to remark that the opposite behavior was observed in the hot weather test. This fact can be related to the lower water solubility shown by additive AAG-02 at 25°C; meanwhile, at 50°C, the solubility difference is inverted.

Finally, the results from Table III show that in cold weather, the film antifog duration increases with vinyl acetate concentration of the polymeric matrix. As FTIR results have not shown significant variations in the additive migration rate, this result could be related to a higher initial additive surface concentration in the films with an increasing percentage of vinyl acetate.

CONCLUSIONS

According to the visual observations, the two additives impart antifog properties to the films in both hot and cold climate conditions, but in all cases, the duration of the effect was longer in the hot-climate test. Although the total concentration of additive decreases with exposure time in the simulated greenhouse, the duration of the antifog effect is directly related to the additive concentration on the film surface. The additives studied in this work show a low migration rate and, therefore, when the antifog effect is lost, important quantities of the additive remain in the bulk.

To achieve a good antifog effect and maintain it during a long time, the antifog additive must have a suitable migration rate and a low solubility in water, resulting in an adequate surface concentration for extended time periods.

References

1. Pieters, J. G. Plasticulture 1996, 112, 23.
2. Turmine, M.; Letellier, P. J Colloid Interface Sci 2000, 227, 71.
3. Howarter, J. A.; Youngblood, J. P. Macromol Rapid Commun 2008, 29, 455.
4. Espí, E.; Salmerón, A.; Fontecha, A.; García, Y.; Real, A. I. J Plast Film Sheet 2006, 22, 85.
5. Földes, E. Die Angew Makromol Chem 1998, 261/262, 65.
6. Lee, K.; Cho, K.; Park, I.; Lee, B. H.; Rana, D.; Choe, S. J Polym Sci Part B: Polym Phys 1999, 37, 1387.
7. Jaffrin, A.; Guion, J. Plasticulture 1994, 102, 41.
8. Földes, E.; Szigeti-Erdei, A. J Vinyl Add Technol 1997, 3, 220.
9. Chalmers, J. M.; Griffiths, P. R. Handbook of Vibrational Spectroscopy, Vol. II; Wiley: Chichester, 2001.
10. Chalmers, J. M.; Griffiths, P. R. Handbook of Vibrational Spectroscopy, Vol. III; Wiley: Chichester, 2001.
11. Zhu, S.; Hirt, D. E. J Vinyl Add Technol 2007, 13, 57.